



General Electric Company 6705 Vallecitos Road, Sunol CA 94586

Non-Proprietary Version

GENE-0000-0043-3105-01 DRF 0000-0043-3105 Class I July 2005

Engineering Report

Quad Cities Unit 2 Replacement Steam Dryer Stress and Fatigue Analysis Based on Measured EPU Conditions



IMPORTANT NOTICE REGARDING THE CONTENTS OF THIS REPORT

Please Read Carefully

Non-Proprietary Notice

This is a non-proprietary version of the document GENE-0000-0043-3105-01-P, which has the proprietary information removed. Portions of the document that have been removed are indicated by an open and closed bracket as shown here [[]].

IMPORTANT NOTICE REGARDING CONTENTS OF THIS REPORT

Please Read Carefully

The only undertakings of the General Electric Company (GENE) with respect to the information in this document are contained in the contract between EXELON and GENE, and nothing contained in this document shall be construed as changing the contract. The use of this information by anyone other than EXELON or for any purpose other than that for which it is intended, is not authorized; and with respect to any unauthorized use, GENE makes no representation or warranty, express or implied, and assumes no liability as to the completeness, accuracy, or usefulness of the information contained in this document, or that its use may not infringe upon privately owned rights.

TABLE OF CONTENTS

Sec	<u>ction</u>	Page
AC	CRONYMS AND ABBREVIATIONS	vi
1.	EXECUTIVE SUMMARY	1
2.	INTRODUCTION AND BACKGROUND	2
	2.1 Dryer Design Bases and Historical Development	2
	2.2 Quad Cities and Dresden EPU Dryer Experience	4
	2.3 Motivation for Additional FIV and Structural Analysis	5
3.	Dynamic Analysis Approach	6
	3.1 Dynamic Loading Pressure Time Histories	6
	3.2 Stress Recovery and Evaluation Methodology	6
4.	Material Properties	7
5.	Design Criteria	7
	5.1 Fatigue Criteria	7
	5.2 ASME Code Criteria for Load Combinations	8
6.	Fatigue Analysis	8
	6.1 Full Dryer Shell Finite Element Model	
	6.2 Dynamic Loads	9
	6.3 Frequency Content of Loads	10
	6.4 Modal Analysis	10
	6.5 Structural Response to Loads	10
	6.6 Stress Results from Time History Analyses	10
	6.7 Weld Factors	13
	6.8 Disposition of High Stress Locations	15
	6.9 Strain Comparison – FEA Results versus Measured Data	16
	6.10 Fatigue Analysis Results	17
7.	ASME Code Load Combinations	21
8.	Conclusions	
9.	References	

ii .

List of Tables

Table 6-1 Shell Element Model Stress Intensity Summa	ry for Time History Cases12
Table 6-2 Maximum Stress Intensity with Weld Factors	14
Table 6-3 Components with High Stress Intensity and I	Disposition15
Table 6-4 Fatigue Analysis Results Summary	
Table 6-5 Comparison of Strain FEA [[]] Results versus Measured Results19
Table 6-5A Comparison of Strain FEA [[]] Results versus Measured Results 20
Table 7-1 ASME Load Combinations	
Table 7-2 ASME Code Cases: Stress Summary Levels .	A and B25
Table 7-2 (cont'd) ASME Code Cases: Stress Summar	y Levels A and B26
Table 7-2 (cont'd) ASME Code Cases: Stress Summary	Level D27
Table 7-2 (cont'd) ASME Code Cases: Stress Summary	Level D28
Table 7-3 ASME Code Margins	

List of Figures

Figure 3-1 ACM Loads: Maximum Applied Pressure	33
Figure 6-1 Replacement Dryer Shell Finite Element Model	34
Figure 6-2 Dryer Finite Element Model Boundary Conditions	
Figure 6-3 Finite Element Model without Super Elements	36
Figure 6-4 ACM Load Frequency Content	37
Figure 6-5 Skirt Frequency: [[]]	38
Figure 6-6 Skirt Frequency: [[]]	39
Figure 6-7 Skirt Frequency: [[]]	.40
Figure 6-8 Skirt Frequency: [[]]	
Figure 6-9 Skirt Frequency: [[]]	.42
Figure 6-10 Skirt Frequency: [[]]	.43
Figure 6-11 Skirt Frequency: [[]]	.44
Figure 6-12 Outer Hood Frequency: [[]]	.45
Figure 6-13 Frequency Response ACM -10%: Hoods	
Figure 6-14 Frequency Response ACM -10%: Vane Bank Ends and Tops, Skirt	.47
Figure 6-15 Frequency Response ACM Nominal: Hoods	.48
Figure 6-16 Frequency Response ACM Nominal: Vane Bank Ends and Tops, Skirt	.49
Figure 6-17 Frequency Response ACM +10%: Hoods	.50
Figure 6-18 Frequency Response ACM +10%: Vane Bank Ends and Tops, Skirt	.51
Figure 6-19 Time History Stress Intensity Results: Vane Cap Flat Portion	.52
Figure 6-20 Time History Stress Intensity Results: Outer Hood	.53
Figure 6-21 Time History Stress Intensity Results: Tie Bars	.54
Figure 6-22 Time History Stress Intensity Results: Frames	.55
Figure 6-23 Time History Stress Intensity Results: Troughs	.56
Figure 6-24 Time History Stress Intensity Results: Gussets	.57
Figure 6-25 Time History Stress Intensity Results: Vane Cap Curved Part	.58
Figure 6-26 Time History Stress Intensity Results: Inner Hoods	.59
Figure 6-27 Time History Stress Intensity Results: Closure Plates	.60
Figure 6-28 Time History Stress Intensity Results: T-Section Webs	.61
Figure 6-29 Time History Stress Intensity Results: T-Section Flanges	.62
Figure 6-30 Time History Stress Intensity Results: Vane Bank Outer End Plates	.63

Figure 6-31 Time History Stress Intensity Results: [[]]64
Figure 6-32 Time History Stress Intensity Results: [[]]65
Figure 6-33 Time History Stress Intensity Results: [[]]66
Figure 6-34 Time History Stress Intensity Results: C	Cross beams67
Figure 6-35 Time History Stress Intensity Results: S	Support Ring68
Figure 6-36 Time History Stress Intensity Results: T	Frough Ledge69
Figure 6-37 Time History Stress Intensity Results: 1	Frough Brace Gusset70
Figure 6-38 Time History Stress Intensity Results: In	nner Trough Brace71
Figure 6-39 Time History Stress Intensity Results: V	
Figure 6-40 Time History Stress Intensity Results: C	Center Support Gussets
Figure 6-41 Time History Stress Intensity Results: C	Center Plate
Figure 6-42 Time History Stress Intensity Results: T	Frough End Stiffeners75
Figure 6-43 Time History Stress Intensity Results: C	Susset Shoe at Cross Beams
Figure 6-44 Time History Stress Intensity Results: F	Frame to Cross Beam Gussets77
Figure 6-45 Time History Stress Intensity Results: L	ifting Rod Guide
Figure 6-46 Locations of Sensors on the FEA Model	I
Figure 6-47 Location of Sensor S7 on the FEA Mod	
Figure 6-48 Strain Gage 1 Comparisons [[]]81
Figure 6-48A Strain Gage 1 Comparisons [[]]82
Figure 6-49 Strain Gage 5 Comparisons [[]]83
Figure 6-49A Strain Gage 5 Comparisons [[]]84
Figure 6-50 Strain Gage 7 Comparisons [[]]85
Figure 6-50A Strain Gage 7 Comparisons [[]]86
Figure 6-51 Strain Gage 8 Comparisons [[]]87
Figure 6-51A Strain Gage 8 Comparisons [[]]88
Figure 6-52 Strain Gage 9 Comparisons [[]]89
Figure 6-52A Strain Gage 9 Comparisons [[]]90
Figure 6-53: Weld Factors to use with Finite Element	nt Results91

v

ACRONYMS AND ABBREVIATIONS

Item	Short Form	Description
1	ACM	Acoustic Circuit predicted pressure loads based on Measurements
		taken from main steam line strain gages (post installation of
		replacement dryer)
2	ASME	American Society of Mechanical Engineers
3	BWR	Boiling Water Reactor
4	EPU	Extended Power Uprate
5	FEA	Finite Element Analysis
6	FEM	Finite Element Model
7	FFT	Fast Fourier Transform
8	FIV	Flow Induced Vibration
9	GE	General Electric
10	GENE	General Electric Nuclear Energy
11	Hz	Hertz
12	IGSCC	Intergranular Stress Corrosion Cracking
13	Mlbm/hr	Millions pounds mass per hour
14	MS	Main Steam
15	MSL	Main Steam Line
16	MWt	Megawatt Thermal
17	NA	Not Applicable
18	NRC	Nuclear Regulatory Commission
19	OBE	Operational Basis Earthquake
20	OLTP	Original Licensed Thermal Power
21	Pb	Primary Bending Stress
22	Pm	Primary Membrane Stress
23	psi	Pounds per square inch
24	Ref.	Reference
25	RMS	Root-Mean-Squared
26	RPV	Reactor Pressure Vessel
27	SCF	Stress Concentration Factor
28	SRSS	Square Root Sum of Squares
29	SRV	Safety Relief Valve

vi

1. EXECUTIVE SUMMARY

In 2002 Quad Cities Unit 2 first developed fatigue cracks in the cover plate portion of the steam dryer after the plant had been operating at extended power uprate (EPU). The result of the root cause evaluation showed the primary factor for this event was high cycle loadings on the dryer. Additional fatigue cracking was observed in 2003 and 2004 in the cover plate and outer hood portions of the repaired Quad Cities and Dresden steam dryers. A replacement dryer was designed to withstand these flow induced vibration loads. The design loads for the replacement dryer were based on time history analyses using acoustic circuit loads from both in-plant steam line data and scale model test (SMT) data. The results of the analyses performed using the design loads are in Reference 17, which established that the replacement dryer components are not vulnerable to fatigue at EPU conditions.

As part of the replacement dryer program, the replacement dryer and main steamlines in Unit 2 were instrumented for the purpose of measuring the pressure loads acting on the dryer. This report summarizes the structural analysis performed to demonstrate the adequacy of the replacement steam dryer design using CDI predicted loads based on main steam line strain gage measurements obtained during the Unit 2 startup with the replacement dryer.

Finite element analyses were performed using a full three-dimensional model of the Exelon replacement dryer comprised of shell elements to determine the most highly stressed locations associated with EPU. The analyses consisted of time history dynamic analyses, frequency calculations, and stress and fatigue analyses. The acoustic circuit model by Continuum Dynamics Inc. (CDI) which was driven by strain gauge measurements on the main steamlines, was used to develop the dryer pressure loads for the time history analyses. In addition, ASME Code based load combinations were also analyzed using the finite element model. Where necessary, the locations of high stress identified in the time history analyses were further evaluated using solid finite element models to more accurately predict the stresses at these locations. Also, in-plant start-up strain measurements on the dryer were compared to FEA results to further confirm the adequacy of the design.

This report summarizes the dynamic, stress and fatigue analyses that demonstrate the Exelon replacement steam dryer is structurally adequate for EPU conditions based on plant measurements taken at Quad Cities Unit 2 during EPU operation of the replacement dryer. The replacement dryer satisfies both the fatigue limit and the ASME Code limits for normal, upset and faulted events at EPU conditions [1].

2. INTRODUCTION AND BACKGROUND

2.1 Dryer Design Bases and Historical Development

The function of the steam dryer is to remove any remaining liquid in the steam exiting from the array of axial flow steam separators. GE BWR steam dryers use commercially available modules of dryer vanes that are enclosed in a GE designed housing to make up the steam dryer assembly. The modules or subassemblies of dryer vanes, called dryer units, are arranged in parallel rows called banks. Four to six banks are used depending on the vessel size. Dryer banks are attached to an upper support ring, which is supported by four to six steam dryer support brackets that are welded attachments to the RPV. The steam dryer assembly does not physically connect to the shroud head and steam separator assembly and it has no direct connection with the core support or shroud. A cylindrical skirt attaches to the upper support ring and projects downward forming a water seal around the array of steam separators. Normal operating water level is approximately mid-height on the dryer skirt. During refueling the steam dryer rests on the floor of the equipment pool on the lower support ring that is located at the bottom edge of the skirt. Dryers are installed and removed from the RPV using the reactor building crane. A steam separator and dryer strongback, which attaches to four steam dryer lifting rod eyes, is used for lifting the dryer. Guide rods in the RPV are used to aid dryer installation and removal. BWR steam dryers typically have guide channels or upper and lower guides that interface with the guide rods.

Wet steam flows upward from the steam separators into an inlet plenum, horizontally through the dryer vane banks, vertically in an outlet plenum and into the RPV dome. Steam then exits the reactor pressure vessel (RPV) through steam outlet nozzles. Moisture (liquid) is separated from the steam by the vane surface and the hooks attached to the vanes. The captured moisture flows downward under the force of gravity to a collection trough that carries the liquid flow to drain pipes and vertical drain channels. The liquid flows by gravity through the vertical drain channels to the lower end of the skirt where the flow exits below normal water level. The outlet of the drain channels is below the water surface in order to prevent reentrainment of the captured liquid.

GE BWR steam dryer technology evolved over many years and several product lines. In earlier BWR/2 and BWR/3 dryers, the active height of the dryer vanes was set at 48 inches. In BWR/4 and later steam dryer designs the active vane height was increased to 72 inches. Perforated plates were included on the inlet and outlet sides of the vane banks of the 72-inch height units in order to distribute the steam flow uniformly through the bank. The addition of perforated plates resulted in a more

uniform velocity over the height of the vanes. The performance for BWR/4 and dryer designs was established by testing in steam. The replacement dryer designed for Quad Cities and Dresden incorporates the performance features of the latest steam dryer designs along with structural design enhancements to better withstand the pressure loading that can result in fatigue crack initiation.

Most of the steam dryer is located in the steam space, with the lower half of the skirt extending below normal water level. These environments are highly oxidizing. All of the BWR/2-6 steam dryers are welded assemblies constructed from Type 304 stainless steel. The Type 304 stainless steel used in BWR/2-6 steam dryers was generally purchased with a maximum carbon content specification of 0.08% (typical ASTM standard). Therefore, the weld heat affected zone material is likely to be sensitized during the fabrication process making the steam dryer susceptible to intergranular stress corrosion cracking (IGSCC). Temporary welded attachments may have also been made to the dryer material that could result in unexpected weld sensitized material. Steam dryer parts such as support rings and drain channels were frequently cold formed, also increasing IGSCC susceptibility. Many dryer assembly welds included crevice areas at the weld root, which were not sealed from the reactor environment. Cold formed 304 stainless steel dryer parts were generally not solution annealed after forming and welding. Because of the environment and material conditions, most steam dryers have exhibited IGSCC cracking. The replacement dryer design specified materials and fabrication processes that will reduce the susceptibility of the dryer to IGSCC cracking compared to the original dryer.

Average steam flow velocities through the dryer vanes at OLTP conditions are relatively modest (2 to 4 feet per second). However, the outer hoods near the steam outlet nozzles are continuously exposed to steam flows in excess of 100 feet per second. These steam velocities have the potential for exciting acoustic resonances in the steam dome and steamlines, provided appropriate conditions exist, resulting in fluctuating pressure loads that act on the dryer.

The dryer is a Class I Seismic but non-safety related component and performs no safety functions. The steam dryer assembly is classified as an "internal structure" per ASME Boiler and Pressure Vessel Code, Section III, Subsection NG. Therefore the steam dryer needs only to be analyzed for those faulted load combinations for which loss of structural integrity of the steam dryer could interfere with the required performance of safety class equipment (i.e., generation of loose parts that may interfere with closure of the MSIVs) or affect the core support structure integrity (shroud, top guide, core support and shroud support).

2.2 Quad Cities and Dresden EPU Dryer Experience

Exelon has experienced dryer cracking and failures at each of the Quad Cities and Dresden units following implementation of EPU. The first dryer failure, loss of the lower horizontal cover plate at Quad Cities Unit 2, occurred in June 2002 after about three months of EPU operation. The root cause of this failure was determined to be high cycle fatigue due to a high frequency fluctuating pressure load. The second dryer failure, also at Quad Cities Unit 2, occurred in May 2003 after a little more than a year of total EPU operation. This failure consisted of severe through-wall cracking in the outer hood, along with cracking of vertical and diagonal internal braces and tie bars. The root cause of this failure was determined to be high cycle fatigue due to fluctuating pressure loads [[

]] The internal gussets for the diagonal braces created a local stress concentration where the fatigue cracking had initiated. Hood cracking was observed at all four outer hood gusset locations. In October 2003, the dryer at Dresden Unit 2 was inspected following a full two year cycle at EPU conditions. Incipient cracking was observed in the outer hoods at all four diagonal brace gusset locations. In November 2003, Quad Cities Unit 1 experienced a hood failure similar to the one that occurred in May 2003 at Quad Cities Unit 2, again after about a year of EPU operation. Following this failure, Dresden Unit 3, which had been operating at EPU for a little more than one year, was shut down and the dryer inspected. Dresden Unit 3 exhibited the same incipient cracking at the outer hood gusset locations as was observed in Dresden Unit 2. In all of these cases, the root cause was determined to be high cycle fatigue due to the fluctuating pressure loads at EPU conditions.

Cracking has also been observed in some of the repairs and modifications that were made to the dryers following these failures. This type of cracking has also been observed to varying degrees in the dryers in all four units. During the March 2004 refueling outage, inspection of the repairs in the Quad Cities Unit 2 dryer showed cracking in the hood plate at the tips of the external gussets on the outer hoods. In November 2004, cracking was observed at one end of the weld between the lower horizontal cover plate and support ring in the Dresden Unit 3 dryer. The lower horizontal cover plate had been replaced in response to the initial 2002 Quad Cities failure as part of the EPU modifications for the dryer. In November 2004, an inspection of the Dresden Unit 2 dryer revealed cracking in the same lower horizontal cover plate weld, this time near the base of one of the external gussets. Recently, a crack was found in this same weld at Quad Cities Unit 1 during a March 2005 inspection, again at the base of one of the external gussets. This cracking experience highlighted the importance of local stress concentrations in determining the fatigue life of the structure. In addition, several of the dryers are beginning to experience fatigue cracking in the perforated plate inserts installed in each dryer as part of the EPU implementation modifications. Tie bar repairs have also experienced cracking.

This experience demonstrates the uncertainty in the useful life of the repairs and modifications performed on the original Quad Cities and Dresden steam dryers.

2.3 Motivation for Additional FIV and Structural Analysis

The experiences at Quad Cities and Dresden demonstrated the need to better understand the nature of the loading and the dynamic structural response of the steam dryers during normal operation. The expense involved with inspection and repair of the dryers for the extended life of the plants provide motivation for determining the loads acting on the dryers and quantifying the stresses in the dryers at EPU conditions. GE and Exelon have initiated development programs to determine the fluctuating pressure loads acting on the dryer in order to confirm the continued acceptability of operating the current dryers and for use in designing a replacement dryer that will be able to accommodate the loading during EPU operation without experiencing cracking.

Based on these needs, this evaluation was initiated to perform the comprehensive structural assessment for the replacement dryer design to assure that it could operate at EPU conditions. The loads affecting the steam dryer were determined and used as input to a three-dimensional finite element model of the Exelon replacement steam dryer. Loads considered in the assessment included steady state pressure, fluctuating, and transient loads, with the primary interest in the steady state fluctuating loads that affect the fatigue life of the dryer. Additionally, ASME-based design load combinations were evaluated for normal, upset and faulted service conditions. A detailed finite element analysis using the dryer model subjected to these design loads was also performed. The analytical results identified the peak stresses and their locations. The results of the analysis also included the analytically determined structural natural frequencies for the different key components and locations in the dryer. Hammer tests were performed on the assembled dryer both dry and in water with varying water elevations. Frequencies from the hammer tests compared well with the finite element model frequencies and showed that no changes were required in the model.

The replacement dryer design has incorporated several design features that reduce the likelihood of fatigue cracking [3, 4]. These features include moving welds out of high stress locations, reducing the number of fillet welds and increasing the number of full penetration welds, and allowing more flexibility in the tie bar attachments to the dryer banks. This report summarizes the dynamic, stress and fatigue analyses performed based on the in-plant load measurements to demonstrate that this new dryer design is structurally adequate for EPU conditions.

3. Dynamic Analysis Approach

3.1 Dynamic Loading Pressure Time Histories

The primary dynamic loads of concern on the dryer are the fluctuating pressure loads during normal operation. The fluctuating pressure loads are responsible for the fatigue damage experienced by the original and repaired steam dryers at all four Dresden and Quad Cities plants. As part of the replacement dryer program, the replacement dryer and main steamlines in Unit 2 were instrumented for the purpose of better defining the pressure loads acting on the dryer. Pressure measurements from the steamlines (inferred from strain gauge measurements on the piping) were used in CDI's acoustic circuit model to estimate the pressures acting on the dryer [5]. These measurements were taken at a power level of 2885 MWt. This load definition is basically the same as the "in-plant" load case in Reference 17; however, the steamline strain gauge placement was improved to provide a more accurate determination of the pressure in the steamline and the acoustic circuit model was refined based on the pressures measured by sensors mounted directly on the steam dryer. Additional details on the CDI acoustic circuit model are provided in Reference 5. The pressure predicted from the CDI acoustic circuit model were applied as time history forcing functions to the structural finite element shell model of the dryer (Figure 3-1).

3.2 Stress Recovery and Evaluation Methodology

The entire shell finite element model was divided into components with every element assigned to a component. An ANSYS macro was written to sweep through each time step on every component to determine the time and location of the maximum stress intensity. [[

]] ANSYS maximum stress intensity results from this macro are presented in Table 6-1. In most cases these stresses from the shell finite element model meet the GENE fatigue design criteria of 10800 psi [1, 7]. In some locations that do not meet this criteria, solid element finite element models from Reference 17 are used and combined with hand calculations to determine more accurate stresses (Table 6-3). Cross beam and support ring high stresses are due to the coarse shell mesh in these locations resulting in overly conservative results. Solid models [17] were used to better characterize the stress state using forces and moments extracted from the shell model. Solid modeling of the weld attachment to the support ring gave a better representation of the local weld geometry and flexibility, thus alleviating the high stresses.

At high stress locations away from the outer hood, an alternate criteria was used as described in Section 5.1. [[

]]

4. Material Properties

The dryer assembly was manufactured from solution heat-treated Type 316L and 304L conforming to the requirements of the material and fabrication specifications [3]. ASME material properties were used [8]. The applicable properties are shown in Table 4-1.

Material / property	Room temperature 70°F	Operating temperature 545°F
SS304L	· · · · · · · · · · · · · · · · · · ·	· · ·
S _v , Yield strength, psi	25000	15940
S _u , Ultimate strength, psi	70000	57440
E, Elastic modulus, psi	28300000	25575000
SS316L	······································	· · · ·
S _v , Yield strength, psi	25000	15495
S _u , Ultimate strength, psi	70000	61600
E, Elastic modulus, psi	28300000	25575000

Table 4-1 Properties of SS304L and SS316L [Reference 8]

5. Design Criteria

5.1 Fatigue Criteria

The fatigue evaluation consists of calculating the alternating stress intensity from FIV loading at all locations in the steam dryer structure and comparing it with the allowable design fatigue threshold stress intensity. The recommended fatigue threshold stress intensities which were developed specifically for the replacement dryer are the following [7]:

1) The acceptable conservative fatigue threshold value of 10,800 psi is to be used as the baseline criterion. It should be used at all critical locations that include the outer hood as the maximum acceptable value for the stress intensity amplitude.

2) The higher ASME Code Curve C value of 13,600 psi may be used in specific cases. However, its use must be technically justified.

The fatigue design criteria for the dryer is based on Figure I-9.2.2 of ASME Section III [9] which provides the fatigue threshold values for use in the evaluation of stainless steels. A key component of the fatigue alternating stress calculation at a location is the appropriate value of the stress concentration factor. The shell finite element model of the full dryer is not capable of predicting the full stress concentrations in the welds. Therefore, additional weld factors are applied to the maximum stress intensities obtained from the shell finite element time history analyses at all weld locations [10]. The stress intensities with the applied weld factors are then compared to the fatigue criteria given above.

5.2 ASME Code Criteria for Load Combinations

The ASME Code stress limits are listed in Table 5-1.

Service level	Stress category	Class 1 Components	: Stress limits (NB)
Service levels A & B	P _m	S _m	Stress Limit, KSI 14.4
	Pm + Pb	1.5S _m	21.6
Service level D	Pm	$Min(.7S_u \text{ or } 2.4 S_m)$	34.56
	$P_m + P_b$	1.5(P _m Allowable)	51.84

Table 5-1 ASME Code Stress Limits [9]	T	able	: 5-1	ASME	Code Stress	Limits [9]
---------------------------------------	---	------	-------	------	-------------	----------	----

Legend:

P_m: General primary membrane stress intensity

P_b: Primary bending stress intensity

S_m: ASME Code stress intensity limit

S_U: Ultimate strength

6. Fatigue Analysis

Time history analyses were performed using ANSYS Version 8.1 [11]. The direct integration time history method was used for all of the cases described in this report. [[

A Rayleigh damping of 2% was used in all of the time history analyses. This was justified based on Reference 19. Knowledge of the significant frequencies that contribute to the total response is used to define the appropriate alpha and beta Rayleigh damping coefficients for the time history direct integration finite element analyses. [[

]]

18 and the hammer test results [12].

]] This is justified based on Reference

6.1 Full Dryer Shell Finite Element Model

The three-dimensional shell model of the replacement dryer is shown in Figures 6-1 through 6-3. The model incorporates super elements for the vane banks, submerged portion of the skirt and tie bar supports. [[

]] The details of the finite element model and associated super elements are contained in Reference 17.

6.2 Dynamic Loads

II

The primary dynamic loads of concern are the fluctuating pressure loads during normal operation. These are the loads responsible for the fatigue damage experienced by all four of the Dresden and Quad Cities steam dryers. As described in Section 3.1, pressure measurements from the steamlines (inferred from strain gauge measurements) were used in CDI's acoustic circuit model to estimate the pressures acting on the dryer [5]. Figure 3-1 shows the applied load at the time when the pressure is a maximum.

Note, the loads used in this analysis were based on measurements taken at a power level of 2885 MWt which is below the EPU power level of 2957 MWt. Consequently, the resulting stress results have been conservatively increased by 10% to account for extension to EPU. [[

6.3 Frequency Content of Loads

The frequency content of the Quad Cities in-plant loads is shown in Figure 6-4. The dryer is symmetric but the loading is asymmetric. [[

]]

6.4 Modal Analysis

Frequency calculations were performed in Reference [17] with the dryer supported from the RPV dryer support brackets. The support was modeled by fixing all translational degrees of freedom at the dryer support bracket interface. The entire dryer was surveyed for the component natural frequencies. However, the focus of the assessment was on the outer dryer surfaces. These calculated component natural frequencies for the skirt are shown in Figures 6-5 through 6-11. [[

]]

6.5 Structural Response to Loads

Structural frequency response for selected components in the dryer [[]] are shown in Figures 6-13 through 6-18. [[

]]

6.6 Stress Results from Time History Analyses

Maximum stress intensity results from ANSYS for all components of the dryer are shown in Table 6-1 [[

]] and plotted in Figures 6-19 through

6-46. [[

]]

Note, the loads used in this analysis were based on measurements taken at a power level of 2885 MWt which is below EPU power level of 2957 MWt. Consequently, the resulting stress results have been conservatively increased by 10% to account for extension to EPU. [[

 Table 6-1 Shell Element Model Stress Intensity Summary for Time History Cases

12

]]

6.7 Weld Factors

The calculation of fatigue alternating stress using the prescribed stress concentration factors in Subsection NG is straightforward when the nominal stress is calculated using the standard strength of material formulas. However, when a finite element analysis (FEA) approach is used, the available stress component information is very detailed and requires added guidance [10] for determining a fatigue stress intensity to be used in conjunction with the ASME Code S-N design curve. The replacement steam dryer welds are analyzed using FEA. Reference 10 provides the basis for calculating the appropriate fatigue factors for use in the S-N evaluation to assess the adequacy of these welds based on the FEA results. Figure 6-53 summarizes the Reference 10 criteria. For the case of full penetration welds, the recommended SCF value is 1.4. In this case, the finite element stress is directly multiplied by the appropriate SCF to determine the fatigue stress. The recommended SCF is 1.8 for a fillet weld when the FEA maximum stress intensity is used. Various studies have shown that the calculated fatigue stress using this alternate approach at a fillet weld correlates with that using a nominal stress and a SCF of 4.0 [14]. An alternative approach involves extracting forces and moments from the shell finite element model near the weld and calculating a nominal stress. This nominal stress would then have a factor of 4.0 applied for a fillet weld. Figure 6-89 shows a chart [[

]]

Note that the above discussion of stress concentration effects (SCF's, fatigue factors, weld factors) only applies to the fatigue evaluation. SCF, "fatigue factor," and "weld factor" are used interchangeably. These terms do not refer to 'weld quality factors' from ASME Subsection NG for primary stress evaluation used in Section 7.0 of this report.

Table 6-2 Maximum Stress Intensity with Weld Factors

[[

14

Table 6-3 Components with High Stress Intensity and Disposition

6.8 Disposition of High Stress Locations

The high stress components for ACM Load Combinations requiring special disposition are summarized in Table 6-3. Details of the disposition are described as follows:

[[

]] Therefore, the cross beams and support

ring are considered acceptable.

6.9 Strain Comparison – FEA Results versus Measured Data

The replacement steam dryer was installed during outage Q2P03 and instrumented. Strain gage data was recorded at various power levels (up to 2885 MWt) during the start up and documented in Reference 22. [[

]]

Table 6-5 shows the rms values of micro-strain for the [[]] strain gages on the dryer that were above the water line and were functioning for the entire start-up including TC-41 at 2885 MWt [5]. The peak values are also provided. Figures 6-48 through 6-52 display the strain time histories along with strain FFTs indicating the frequency response. The mounted direction of the strain gages is shown in the first column of Table 6-5. Plots of FEA strain results are consistent with the mounting direction of the gages.

Results appear to correlate well in both magnitude and frequency content between the measured data and the data from the finite element analysis [[

16

Note the strains in the dryer skirt at S-8 are very conservative from the analysis. Thus it is expected the stress results for the dryer skirt are also conservatively calculated. There is significant conservatism in the loads analysis for the skirt. The hammer tests [12] confirmed the reasonableness of the structural model.

6.10 Fatigue Analysis Results

The fatigue analysis results are a compilation of shell finite element model, solid model, and manual calculations for assessing the acceptability of the steam dryer against the fatigue design criteria. [[

]] The maximum stresses directly from the ANSYS shell finite element analysis are summarized in Table 6-1. The stresses [[

]] are summarized in Table 6-2. The components requiring additional evaluations are summarized in Table 6-3. The fatigue evaluation results including use of previous solid models [17], different damping values, and an alternate fatigue limit in areas away from the outer hood are summarized in Table 6-4. All components listed meet the fatigue design allowables.

Additionally, the measured strain data on the dryer taken during plant start up appears to correlate well with the ANSYS results, providing additional assurance in the conclusions of the pre-installation dryer design basis report [17].

Table 6-4 Fatigue Analysis Results Summary

]]

 Table 6-5 Comparison of Strain FEA [[

 Results

]] Results versus Measured

[[

Table 6-5A Comparison of Strain FEA [[Measured Results

]]

]] Results versus

7. ASME Code Load Combinations

The replacement dryer was analyzed in Reference 17 for ASME Code load combinations (primary stresses) as described in Table 7-1. The acceptance criteria used for these evaluations are specified in Section 5.2 and are the same as those used for safety related components. Since the only loads that have changed are the FIV loads, the existing load combinations were evaluated to demonstrate that the allowable stress criteria were still being met with the new (post-installation) FIV loads included. [[

]] In all other cases, since the original loads determined from the pre-installation analysis [17] are greater than the new loads, re-evaluation is not required. [[

]]

]]

]]

 Table 7-3 summarizes the design margins for the highest stresses for each service

 level.
 [[

]] The stress contour for each component was individually evaluated. Where necessary, primary stress was determined for the component and the peak stress in the FIV stress listing was replaced with the lower (and more appropriate) general primary stress value. The values obtained from the stress contour plot were multiplied by a factor of 1.1 to account for full EPU conditions. [[

]]

Table 7-2 gives a stress summary with the ASME Code allowables [[

]] at the bottom of the table for each load combination. Thus the ASME Code Load limits are met. Disposition of all issues with weld inspection records, as documented in the associated DDR's, remains applicable.

The ASME Code combination results are summarized in Table 7-3.

Load Case	Service Condition	Load Combination	Notes
A	Normal	$DW + DPn \pm FIVn$	
B1	Upset	$DW + DPn + TSV1 \pm FIVn$	
B2	Upset	DW + DPn + TSV2	1
B3	Upset	$DW + DPu \pm FIVu$	2
B4	Upset	$DW + DPn \pm OBE \pm FIVn$	
DIA	Faulted	$DW + DPn + [SSE^2 + AC1^2]^{1/2} \pm FIVn$	3
D1B	Faulted	$DW + [DPf1^2 + SSE^2]^{1/2}$	3, 4
D2A	Faulted	$DW + DPn + AC2 \pm FIVn$	
D2B	Faulted	DW + DPf2	4

Table 7-1 ASME Load Combinations

Notes:

- 1. In the Upset B2 combination, FIVn is not included because the reverse flow through the steamlines will disrupt the acoustic sources that dominate the FIVn load component.
- 2. The relief valve opening decompression wave load (acoustic) associated with an inadvertent or stuck-open relief valve (SORV) opening is bounded by the TSV acoustic load (Upset B1); therefore, the acoustic phase of the SORV load need not be explicitly evaluated or included in the Upset load combination B3.
- 3. Loads from independent dynamic events are combined by the square root sum of the squares method.
- 4. In the Faulted D1B and D2B combinations, FIVn is not included because the level swell in the annulus between the dryer and vessel wall will disrupt the acoustic sources that dominate the FIVn load component.
- AC1 = Acoustic load due to Main Steam Line Break (MSLB) outside containment, at the Rated Power and Core Flow (Hi-Power) Condition.
- AC2 = Acoustic load due to Main Steam Line Break (MSLB) outside containment, at the Low Power/High Core Flow (Interlock) Condition.
- DW = Dead Weight

DPn = Differential Pressure Load During Normal Operation

- DPu = Differential Pressure Load During Upset Operation
- DPf1 = Differential Pressure Load in the Faulted condition, due to Main Steam Line Break Outside Containment at the Rated Power and Core Flow (Hi-Power) condition
- DPf2 = Differential Pressure Load in the Faulted condition, due to Main Steam Line Break Outside Containment at the Low Power/High Core Flow (Interlock) condition
- FIVn = Flow Induced Vibration Load (zero to peak amplitude of the response) during Normal Operation
- FIVu = Flow Induced Vibration Load (zero to peak amplitude of the response) during Upset Operation
- OBE = Operating Basis Earthquake
- SSE = Safe Shutdown Earthquake
- TSV1 = The Initial Acoustic Component of the Turbine Stop Valve (TSV) Closure Load (Inward load on the outermost hood closest to the nozzle corresponding to the TSV closure)
- TSV2 = The Flow Impingement Component (following the Acoustic phase) of the TSV Closure Load; (Inward load on the outermost hood closest to the nozzle corresponding to the TSV closure)

Table 7-2 ASME Code Cases: Stress Summary Levels A and B \rightarrow [[]] 25

 Table 7-2 (cont'd)
 ASME Code Cases: Stress Summary Levels A and B

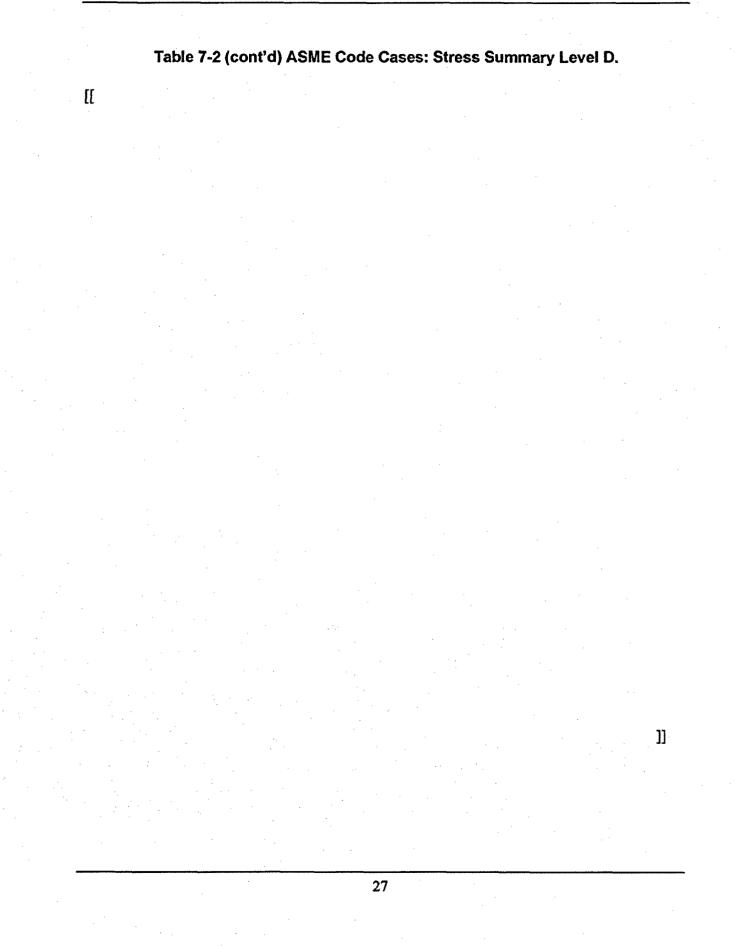
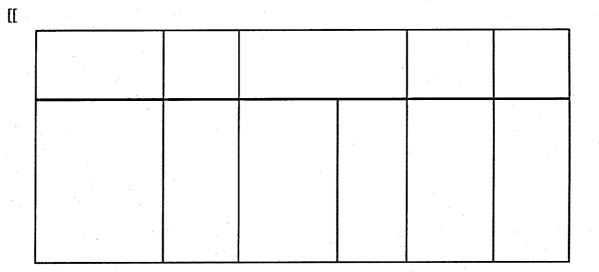


Table 7-2 (cont'd) ASME Code Cases: Stress Summary Level D.]]]] 28

Table 7-3 ASME Code Margins



8. Conclusions

The fatigue evaluation of the dryer was based on time history analyses using predicted loads from the acoustic circuit model based on in-plant steam line data. The loads were run for nominal and +/-10% frequency shifts. Results of all three fluctuating pressure cases show that the replacement dryer is structurally adequate from a fatigue standpoint at EPU conditions. All locations in the steam dryer are below the design fatigue allowable stress limit as defined in the GENE Design Criteria [1]. All stresses from the ASME service level A (normal), B (upset), and D (faulted) loads are within the ASME Code allowable limits for primary stresses. Strain gage measurements on the dryer are in reasonable agreement with the analysis results. Based on these results, the replacement dryer is structurally adequate for EPU conditions.

9. References

- "Steam Dryer Design Specification" (DS) 26A6266, Revision 3; "Design Specification Data Sheet" (DSDS) 26A6266AB, Revision 5.
- [2] CDI: Acoustic Evaluation Modeling and Methodology.
- [3] GENE Material Specification: 26A6273, Revision 4.
- [4] GENE Fabrication Specification: 26A6274, Revision 6.
- [5] Exelon TODI No. QDC-05-028 Rev. 1 "Quad Cities Startup Testing Power Levels for Test Conditions Unit 2 for TC 32/33 & TC41A".
- [6] N/A
- [7] "Fatigue Stress Threshold Criteria for use in the Exelon Replacement Steam Dryer", GENE 0000-0034-8374, October 2004.
- [8] ASME Code, Section II, 1998 Edition with 2000 Addenda.
- [9] American Society of Mechanical Engineers (ASME) Boiler and Pressure Vessel Code, Section III, 1998 Edition with 2000 Addenda.
- [10] "Recommended Weld Quality and Stress Concentration Factors for use in the Structural Analysis of the Exclon Replacement Steam Dryer", GENE 0000-0034-6079, February 2005.
- [11] ANSYS Release 8.1, ANSYS Incorporated, 2002
- [12] "Test and Analysis Report Quad Cities New Design Steam Dryer Dryer #1 Experimental Modal Analysis and Correlation with Finite Element Results," LMS- Engineering Innovation, April 22, 2005
- [13] N/A
- [14] "Exelon Steam Dryer Dynamic Time History Analyses," GENE 0000-0039-3540, April 2005.
- [15] "Exelon Steam Dryer Replacement Program 2% Structural Damping for Seismic and Non-Seismic (FIV) Dynamic Analysis", Letter Report dkh0503, March 18, 2005

- [16] "Quad Cities 1 & 2 Steam Dryer Replacement- 4% Structural Damping for Vane Bank FIV Analysis," GENE 0000-0039-4768, April 21, 2005.
- [17] "Quad Cities Units 1 and 2 Replacement Steam Dryer Analysis Stress, Dynamic, and Fatigue Analyses for EPU Conditions," DRF GE-NE-0000-0034-3781, Section GE-NE-0000-0039-4902, Revision 0, April 2005.
- [18] "Exelon Steam Dryer Replacement 4% Structural Damping for Dryer Skirt FIV Analysis," DRF GE-NE-0000-0039-4747, Section GE-NE-0000-0041-9435, Revision 0, June 2005.
- [19] "Exelon Steam Dryer Replacement 2% Structural Damping Seismic & FIV Loads," DRF GE-NE-0000-0039-4747, Section GE-NE-0000-0039-4749, Revision 1, June 2005.
- [20] "Weld Inspection Calculations for Replacement Dryer," DRF GE-NE-0000-0039-4028, Section GE-NE-0000-0039-4057, Revision 0.
- [21] "Trough Drain Pipe Weld Disposition," DRF GE-NE-0000-0039-4028, Section GE-NE-0000-0039-5878, Revision 0.
- [22] "QC2 Strain Evaluation with 2% Damping," DRF GE-NE-0000-0041-9352, Section GE-NE-0000-0042-4718, Revision 0.
- [23] "QC2 Strain Evaluation with 1% Damping" DRF GE-NE-0000-0041-9352, Section GE-NE-0000-0042-0551, Revision 0.
- [24] "Two Second Internal NRC Explanation," DRF GE-NE-0000-0041-3989, Section GE-NE-0000-0042-2761, Revision 0.
- [25] GE Weld Design Factor Approach (email from Har Mehta, dated 4/12/2005).
- [26] "Additional Justification of Power Law Scaling of Stresses in Quad Cities Unit 2 Steam Dryer to Final EPU Level of 2957 MWt", eDRF 0000-0041-9352, eDRF Section 0000-0043-2935.

32

[[

Figure 3-1 ACM Loads: Maximum Applied Pressure

[[. . .

]]

Figure 6-1 Replacement Dryer Shell Finite Element Model

Figure 6-2 Dryer Finite Element Model Boundary Conditions

Figure 6-3 Finite Element Model without Super Elements

Figure 6-4 ACM Load Frequency Content

[[...

Figure 6-5 Skirt Frequency: [[

]]

[[

Figure 6-6 Skirt Frequency: [[

]]

11

Figure 6-7 Skirt Frequency: [[

]]

ĺ

 Figure 6-8 Skirt Frequency: [[
]]

Figure 6-9 Skirt Frequency: [[

]]

]]

Figure 6-10 Skirt Frequency: [[]]

Figure 6-11 Skirt Frequency: [[

]]

Ì

]]

]]

Figure 6-12 Outer Hood Frequency: [[

45

Figure 6-13 Frequency Response ACM –10%: Hoods

Figure 6-14 Frequency Response ACM –10%: Vane Bank Ends and Tops, Skirt

Figure 6-15 Frequency Response ACM Nominal: Hoods

48

Figure 6-16 Frequency Response ACM Nominal: Vane Bank Ends and Tops, Skirt

Figure 6-17 Frequency Response ACM +10%: Hoods

Figure 6-18 Frequency Response ACM +10%: Vane Bank Ends and Tops, Skirt

ננ

Figure 6-19 Time History Stress Intensity Results: Vane Cap Flat Portion

Figure 6-20 Time History Stress Intensity Results: Outer Hood

Figure 6-21 Time History Stress Intensity Results: Tie Bars

Figure 6-22 Time History Stress Intensity Results: Frames

Figure 6-23 Time History Stress Intensity Results: Troughs

[[

Figure 6-24 Time History Stress Intensity Results: Gussets

[[. .

]]

Figure 6-25 Time History Stress Intensity Results: Vane Cap Curved Part

]]

Figure 6-26 Time History Stress Intensity Results: Inner Hoods

Figure 6-27 Time History Stress Intensity Results: Closure Plates

[[

Figure 6-28 Time History Stress Intensity Results: T-Section Webs

[[. .

]]

Figure 6-29 Time History Stress Intensity Results: T-Section Flanges



Figure 6-31 Time History Stress Intensity Results: [[

]]

Figure 6-32 Time History Stress Intensity Results: [[]]

Figure 6-33 Time History Stress Intensity Results: [[]]

]]

Figure 6-34 Time History Stress Intensity Results: Cross beams

Figure 6-35 Time History Stress Intensity Results: Support Ring

Figure 6-36 Time History Stress Intensity Results: Trough Ledge

]]

Figure 6-37 Time History Stress Intensity Results: Trough Brace Gusset

Figure 6-38 Time History Stress Intensity Results: Inner Trough Brace

[[

]]

Figure 6-39 Time History Stress Intensity Results: Vertical Support Plates

Figure 6-40 Time History Stress Intensity Results: Center Support Gussets

]]

Figure 6-41 Time History Stress Intensity Results: Center Plate

]]

Figure 6-42 Time History Stress Intensity Results: Trough End Stiffeners

Figure 6-43 Time History Stress Intensity Results: Gusset Shoe at Cross Beams

Figure 6-44 Time History Stress Intensity Results: Frame to Cross Beam Gussets

]]

Figure 6-45 Time History Stress Intensity Results: Lifting Rod Guide

Figure 6-46 Locations of Sensors on the FEA Model

[[. .

Figure 6-47 Location of Sensor S7 on the FEA Model

[[

Figure 6-48 Strain Gage 1 Comparisons [[

]]

[[

Figure 6-48A Strain Gage 1 Comparisons [[

]]

]]

Figure 6-49 Strain Gage 5 Comparisons [[

83

]]

]]

Figure 6-49A Strain Gage 5 Comparisons [[

]]

]]

Figure 6-50 Strain Gage 7 Comparisons [[

]]

]]

Figure 6-50A Strain Gage 7 Comparisons [[

]]

]]

Figure 6-51 Strain Gage 8 Comparisons [[

]]

[[

Figure 6-51A Strain Gage 8 Comparisons [[

Л

[[

Figure 6-52 Strain Gage 9 Comparisons [[

]]

П

]]

Figure 6-52A Strain Gage 9 Comparisons [[(

]]

]]]

Figure 6-53: Weld Factors to use with Finite Element Results